Supporting Information

Synthetic and structural studies of mixed sodium bis(trimethylsilyl)amide-sodium halide aggregates in the presence of η^2-*N*,*N*-, η^3-*N*,*N*,*N*/*N*,*O*,*N*- and η^4-*N*,*N*,*N*,*N*-donor ligands

Ana I. Ojeda-Amador, Antonio J. Martínez-Martínez, Alan R. Kennedy and Charles T. O'Hara*

WestCHEM, Department of Pure and Applied Chemistry, University of Strathclyde, Glasgow, G1 1XL, UK

E-mail: charlie.ohara@strath.ac.uk

Table S1. Selected crystallographic and refinement data for co-complexes **1**, **2** and **4**.

Compound	**1**	**2**	**4**
Formula	$C_{21}H_{60}Cl_{0.5}N_{4.5}Na_3Si_5$	$C_{42}H_{120}BrN_9Na_6Si_{10}$	$C_{60}H_{172}IN_{13}Na_8Si_{14}$
Fw	602.88	1250.21	1780.18
Crystal system	Monoclinic	Monoclinic	Triclinic
Space group	P_{21}	P_{21}	P_{-1}
Wavelength/Å	0.71073	0.71073	0.71073
a/Å	13.7203(3)	13.7374(3)	13.3266(4)
b/Å	20.5494(3)	20.6050(3)	19.8058(5)
c/Å	14.5519(2)	14.5508(3)	22.0443(5)
α/°	90	90	87.386(2)
β/°	110.097(2)	110.422(3)	79.156(2)
γ/°	90	90	74.411(3)
Volume/Å^3	3853.01(12)	3859.86(15)	5504.3(3)
Z	4	2	2
Temperature/*K*	123(2)	123(2)	123(2)
Refls. Collect.	47741	40805	77404
$2\theta_{max}$	55.75	60.82	55
R_{int}	0.0281	0.0377	0.0499
Goodness of fit	1.023	0.992	1.033
$R[F^2>2\sigma]$, *F*	0.0319	0.0434	0.0457
R_w (all data), F^2	0.0761	0.0870	0.1054

Table S2. Selected crystallographic and refinement data for co-complexes **5**-**8**.

Compound	**5**	**6**	**7**	**8**
Formula	$C_{46}H_{130}IN_9Na_6O_2Si_{10}$	$C_{38}H_{98}IN_7Na_4Si_6$	$C_{30}H_{86}IN_7Na_4Si_6$	$C_{30}H_{86}BrN_7Na_4Si_6$
Fw	1387.32	1040.63	932.45	885.46
Crystal system	Orthorhombic	Monoclinic	Monoclinic	Monoclinic
Space group	Pca_{21}	P_{21}	$P_{21/n}$	P_n
Wavelength/Å	0.71073	1.54184	1.54184	1.54184
a/Å	19.4798(6)	13.3519(3)	15.2873(6)	9.0031(2)
b/Å	31.7695(3)	15.3554(5)	22.3153(6)	14.65856(18)
c/Å	29.0262(4)	15.3294(4)	17.8166(9)	20.7632(2)
α/°	90	90	90	90
β/°	90	105.646(2)	113.919(5)	93.6525(15)°
γ/°	90	90	90	90
Volume/Å^3	17963.3(6)	3026.44(15)	5556.0(4)	2734.61(8)
Z	8	2	4	2
Temperature/*K*	123(2)	123(2)	123(2)	123(2)
Refls. Collect.	266275	18272	35327	31873
$2\theta_{max}$	60.46	146.51	146.40	139.98
R_{int}	0.0622	0.0426	0.0319	0.0306
Goodness of fit	0.989	1.029	1.042	1.072
$R[F^2>2\sigma]$, *F*	0.0533	0.0462	0.0535	0.0509
R_w (all data), F^2	0.1198	0.1174	0.1694	0.1418

Table S3. ^{1}H and ^{13}C δ for **1**-**5** in d_8-THF at 300 K.

			^{1}H δ d_8-THF	**^{13}C δ d_8-THF**
1	Me_6TREN	CH_2 backbone	2.55, 2.31	58.8, 53.9
		Me	2.16	46.0
	NaHMDS	$SiMe_3$	-0.20	6.6
2	Me_6TREN	CH_2 backbone	2.55, 2.33	58.6, 53.5
		Me	2.18	46.0
	NaHMDS	$SiMe_3$	-0.19	6.6
3	Me_6TREN	CH_2 backbone	2.52, 2.36	58.0, 52.5
		Me	2.23	45.8
	NaHMDS	$SiMe_3$	-0.19	6.6
4	PMDETA	CH_2 backbone	2.42, 2.33	58.6, 57.0
		MeN	2.22	46.2
		Me_2N	2.18	43.5
	NaHMDS	$SiMe_3$	-0.19	6.8
5	TMDAE	CH_2 backbone	3.50, 2.42	69.8, 59.8
		Me	2.20	46.2
	NaHMDS	$SiMe_3$	-0.19	6.8

Table S4. ^{1}H and ^{13}C δ of **5** in d_8-toluene at 363 K.

			^{1}H δ d_8-Toluene	**^{13}C δ d_8-Toluene**
5	TMDAE	CH_2 backbone	2.96, 2.04	67.0, 58.8
		Me	2.00	45.0
	NaHMDS	$SiMe_3$	0.16	7.0

Table S5. ^{1}H and ^{13}C δ 5 of **6-8** in C_6D_6 at 300 K.

			^{1}H δ C_6D_6	^{13}C δ C_6D_6
6	R,R-TMCDA	Me	2.12	41.0
		α-CH_2 backbone	2.00	63.7
		β/γ-CH_2 backbone	1.42	25.3
		β/γ-CH_2 backbone	0.69	21.5
	NaHMDS	$SiMe_3$	0.41	7.5
7	TMEDA	Me	2.00	46.4
		CH_2 backbone	1.82	57.2
	NaHMDS	$SiMe_3$	0.36	7.2
8	TMEDA	Me	1.99	46.2
		CH_2 backbone	1.84	57.2
	NaHMDS	$SiMe_3$	0.35	7.2

Table S6. ^{1}H and ^{13}C δ of the monomeric species NaHMDS·Me_6TREN and NaHMDS·PMDETA in d_8-THF at 300 K.

			^{1}H d_8-THF	^{13}C d_8-THF
NaHMDS·Me_6TREN	Me_6TREN	CH_2 backbone	2.55, 2.30	59.1, 54.3
		Me	2.16	46.3
	NaHMDS	$SiMe_3$	-0.19	6.8
NaHMDS·PMDETA	PMDETA	CH_2 backbone	2.42, 2.31	58.8, 57.3
		N′Me	2.2	43.4
		N,N″Me	2.16	46.2
	NaHMDS	$SiMe_3$	-0.19	6.8

Table S7. ^{1}H δ of the monomeric species NaHMDS·TMDAE in d_8-toluene at 363 K.

			^{1}H d_8-Toluene at 363 K
NaHMDS·TMDAE	TMDAE	CH_2 backbone	3.07 (OCH_2), 2.15 (NCH_2)
		Me	2.08
	NaHMDS	$SiMe_3$	0.19

Table S8. ^{1}H and $^{13}C\{^{1}H\}$ δ of the TMEDA and R,R-TMCDA ligands in C_6D_6 at 273 K.

		^{1}H C_6D_6	^{13}C C_6D_6
R,R-TMCDA	Me	2.29	40.6
	α-CH	2.26	64.3
	β/γ-CH_2 backbone	1.75, 1.60	26.0
	β/γ-CH_2 backbone	1.01, 1.01	25.7
TMEDA	Me	2.12	46.0
	CH_2 backbone	2.36	58.4

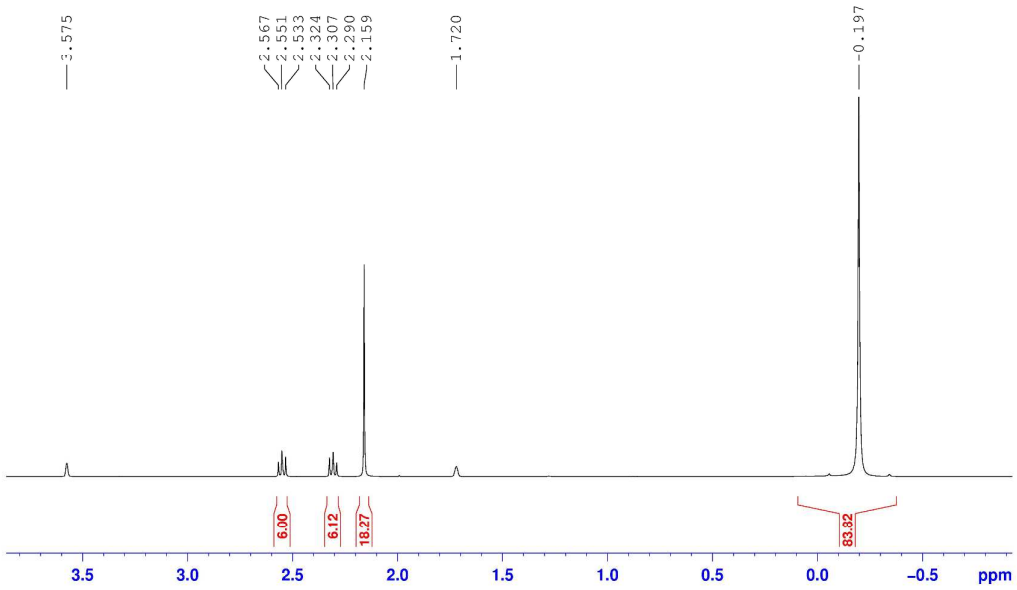

Figure S1. ^{1}H NMR (400.1 MHz, d_8-THF, 300 K) of isolated crystals of **1**.

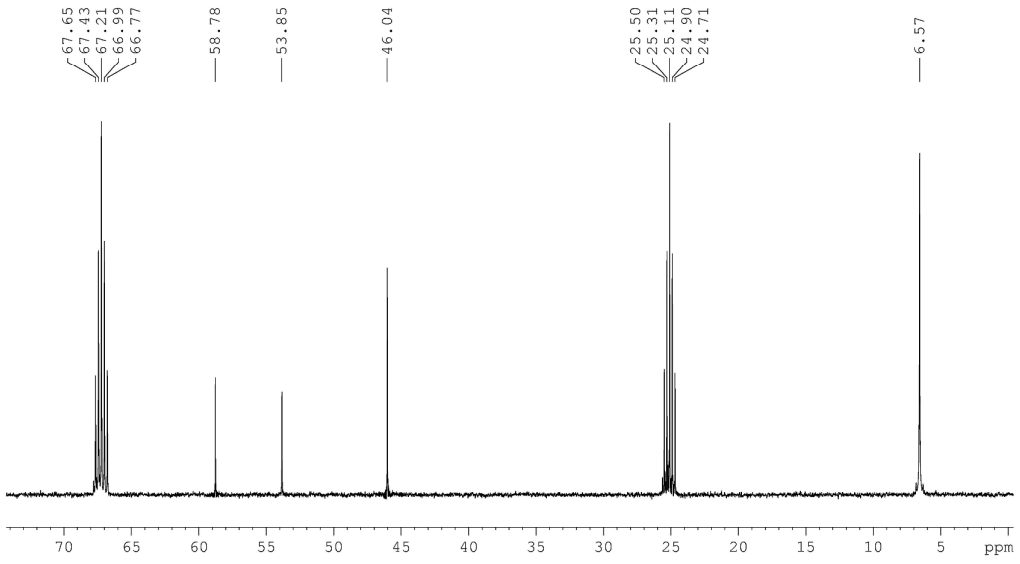

Figure S2. $^{13}C\{^{1}H\}$ NMR spectrum (100.6 MHz, d_8-THF, 300 K) of isolated crystals of **1**.

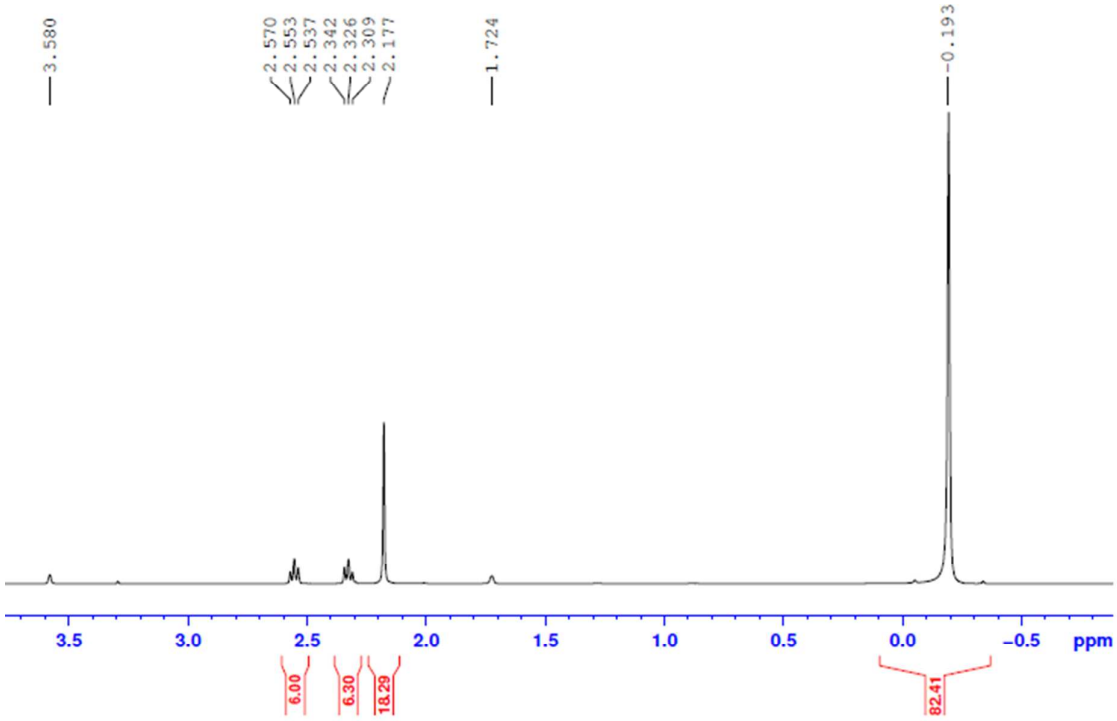

Figure S3. ^{1}H NMR (400.1 MHz, d_8-THF, 300 K) of isolated crystals of **2**.

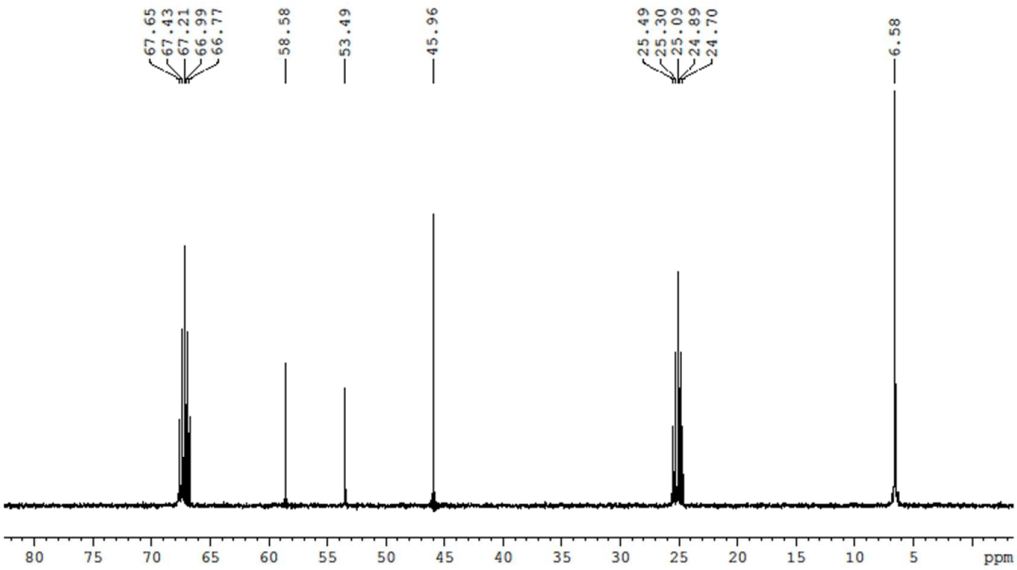

Figure S4. ^{13}C{^{1}H} NMR spectrum (100.6 MHz, d_8-THF, 300 K) of isolated crystals of **2**.

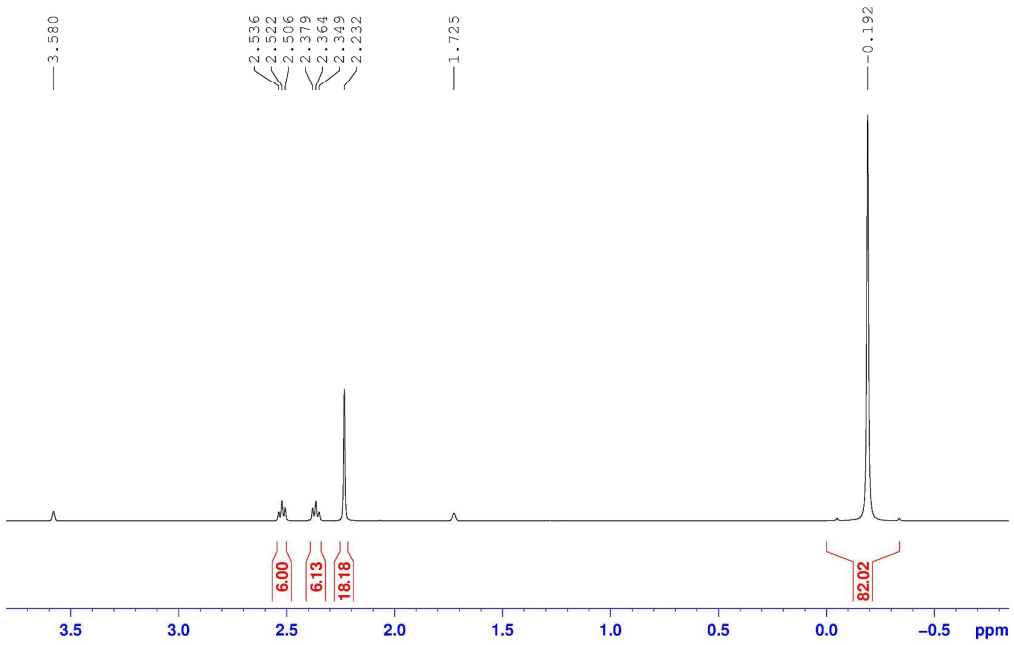

Figure S5. ^{1}H NMR (400.1 MHz, d_8-THF, 300 K) of isolated crystals of **3**.

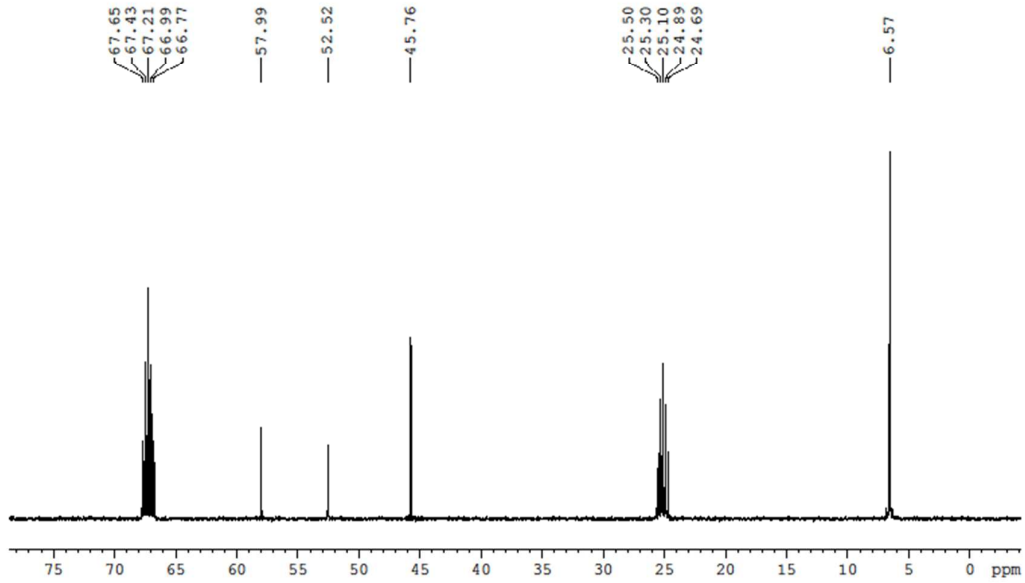

Figure S6. ^{13}C{^{1}H} NMR spectrum (100.6 MHz, d_8-THF, 300 K) of isolated crystals of **3**.

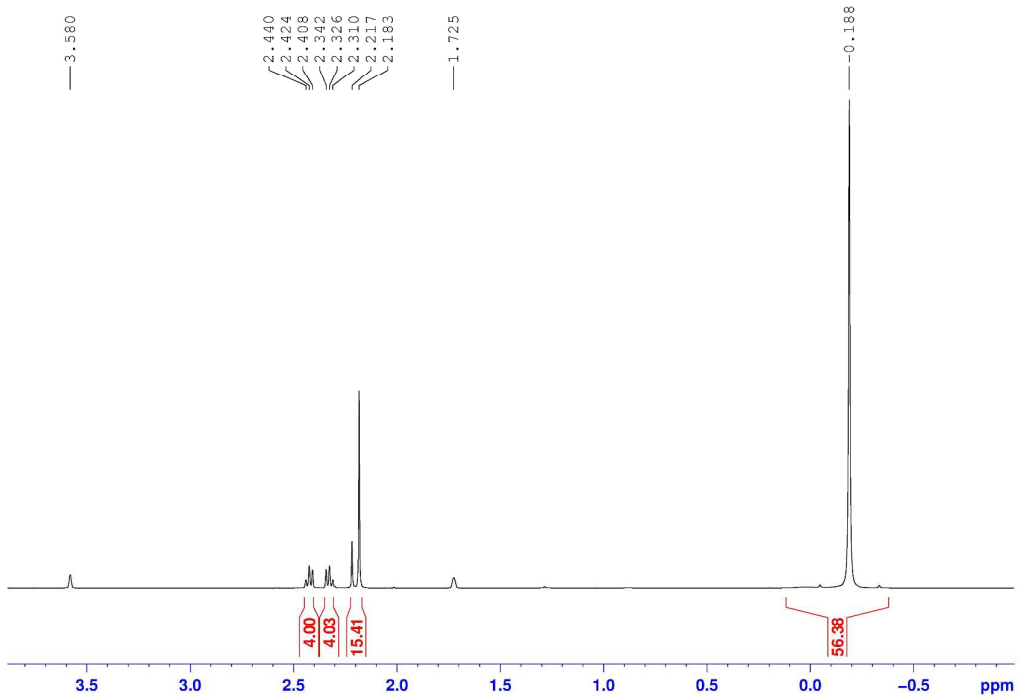

Figure S7. ^{1}H NMR spectrum (400.1 MHz, d_8-THF, 300K) of isolated crystals of **4**.

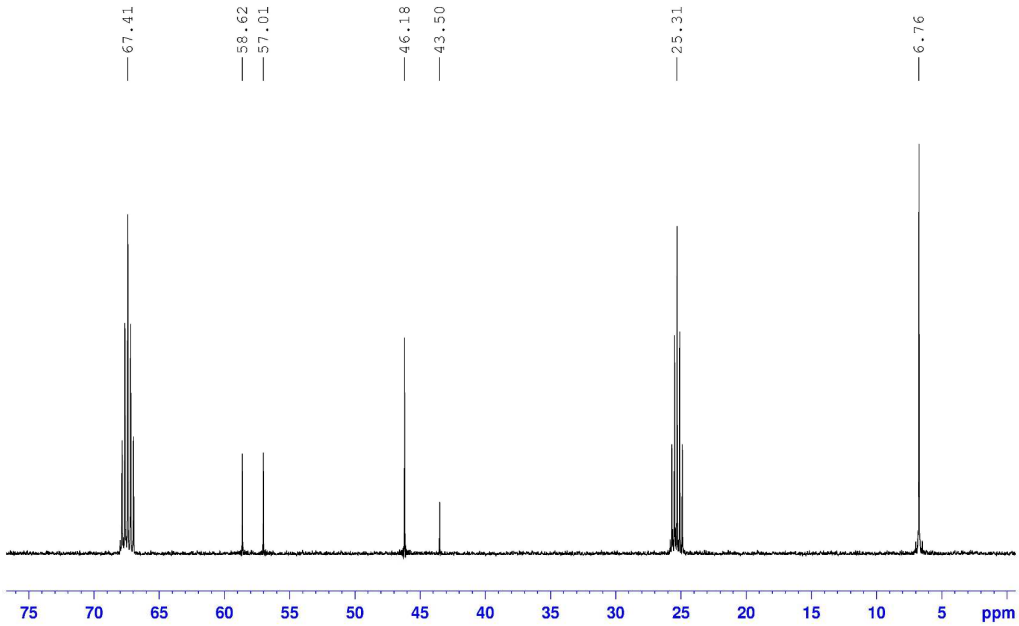

Figure S8. ^{13}C{^{1}H} NMR spectrum (100.6 MHz, d_8-THF, 300K) of isolated crystals of **4**.

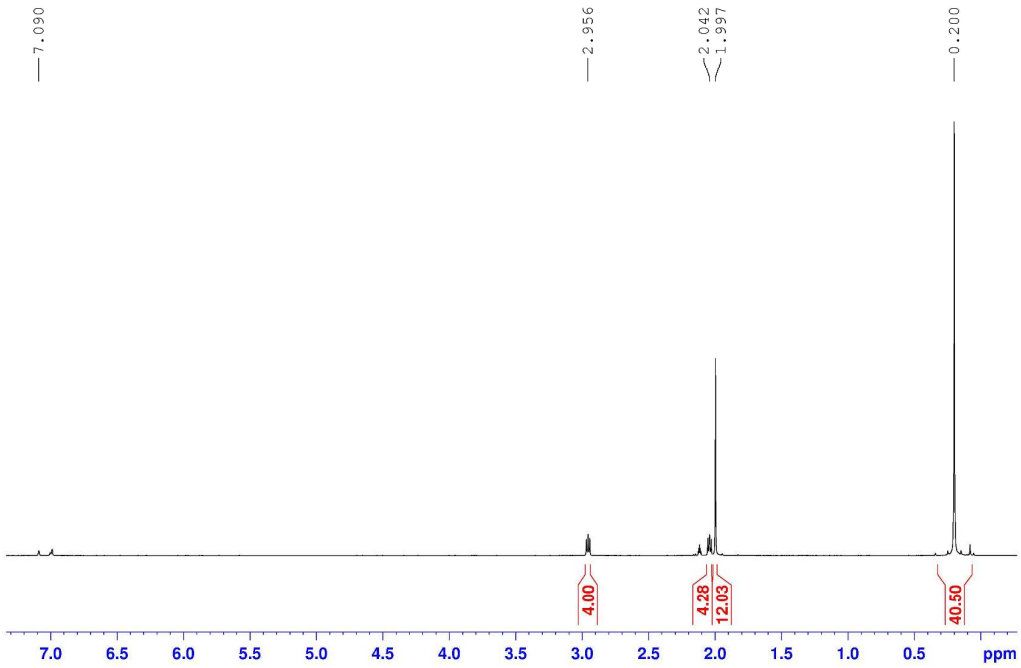

Figure S9. ^{1}H NMR (400.1 MHz, d_8-toluene, 363 K) of isolated crystals of **5**.

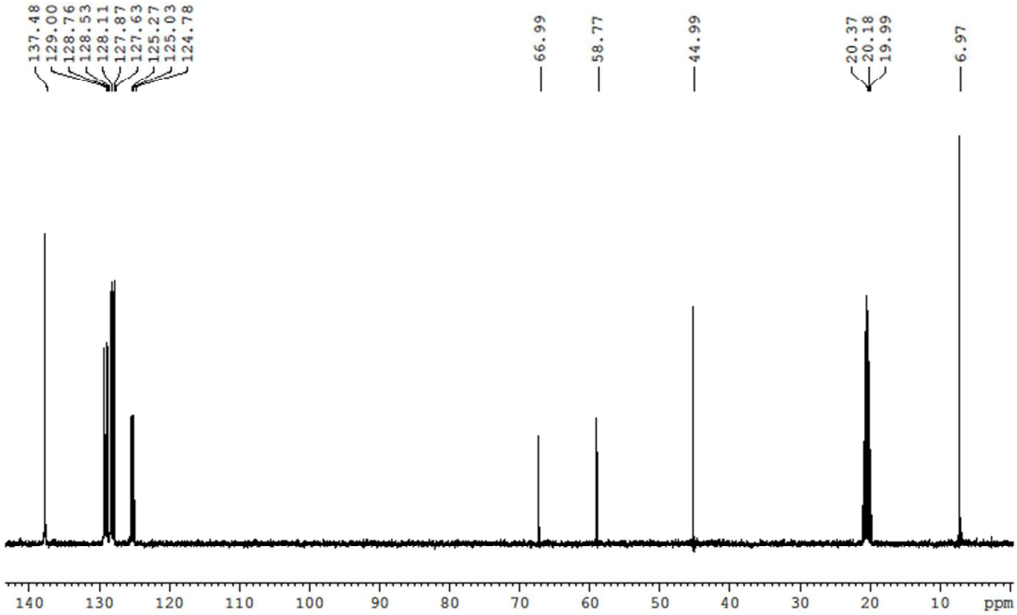

Figure S10. ^{13}C NMR (400.1 MHz, d_8-toluene, 363 K) of isolated crystals of **5**.

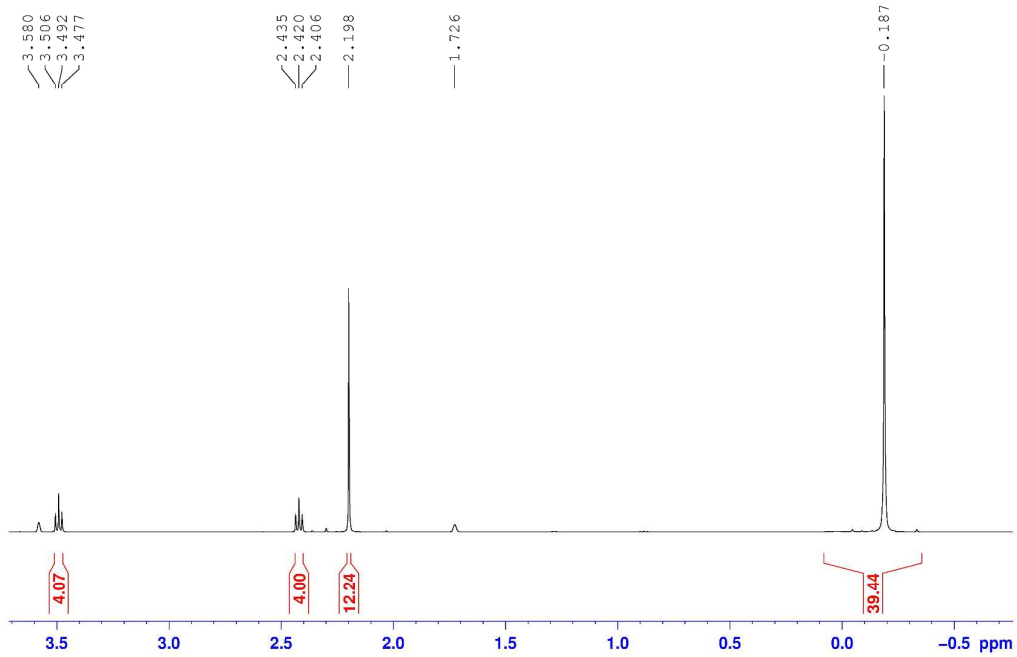

Figure S11. ^{13}H NMR (400.1 MHz, d_8-THF, 363 K) of isolated crystals of **5**.

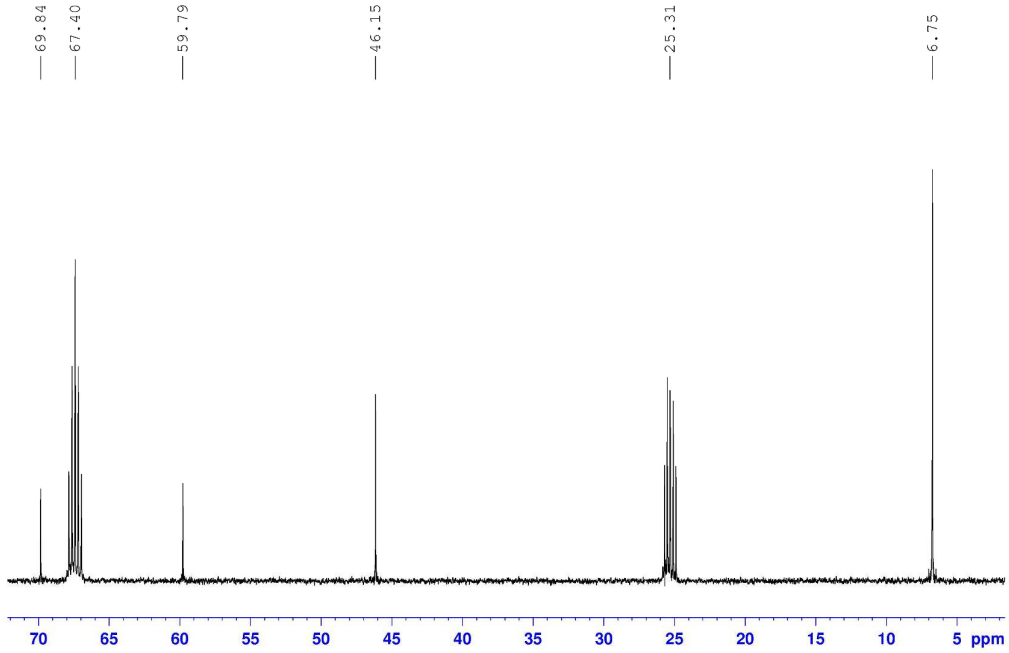

Figure S12. ^{13}C NMR (400.1 MHz, d_8-THF, 363 K) of isolated crystals of **5**.

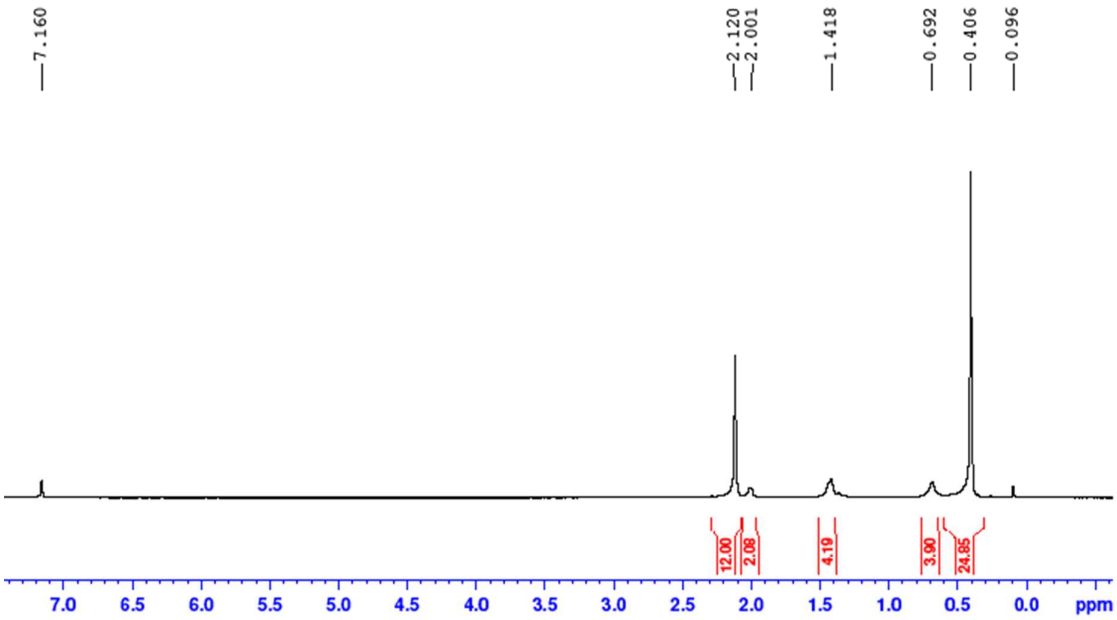

Figure S13. ^{1}H NMR spectrum (400.1 MHz, C_6D_6, 300 K) of isolated crystals of **6**.

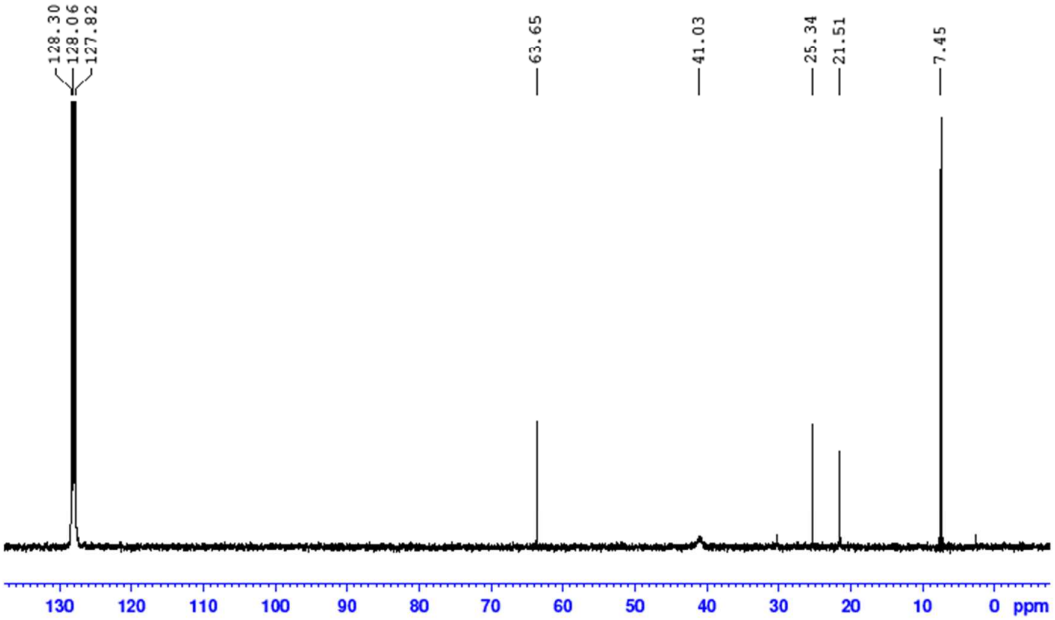

Figure S14. ^{13}C{^{1}H} NMR spectrum (100.6 MHz, C_6D_6, 300 K) of isolated crystals of **6**.

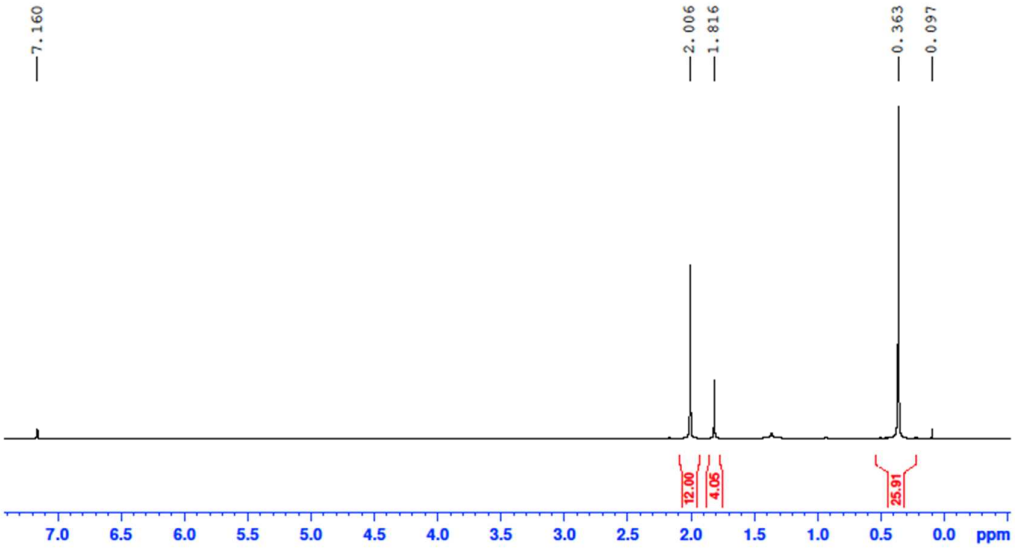

Figure S15. ^{1}H NMR spectrum (400.1 MHz, C_6D_6, 300 K) of isolated crystals of **7**.

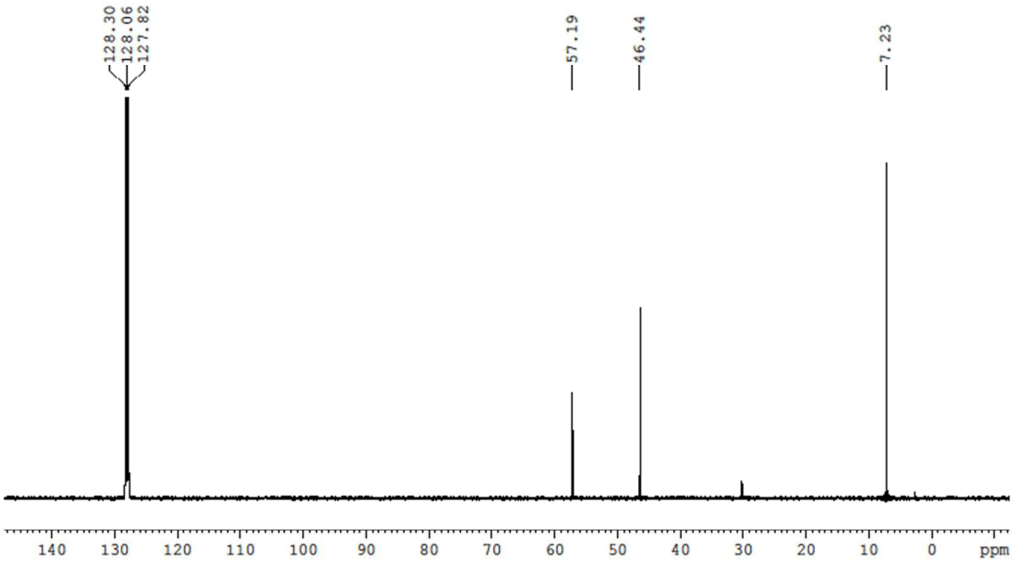

Figure S16. ^{13}C{^{1}H} NMR spectrum (100.6 MHz, C_6D_6, 300 K) of isolated crystals of **7**.

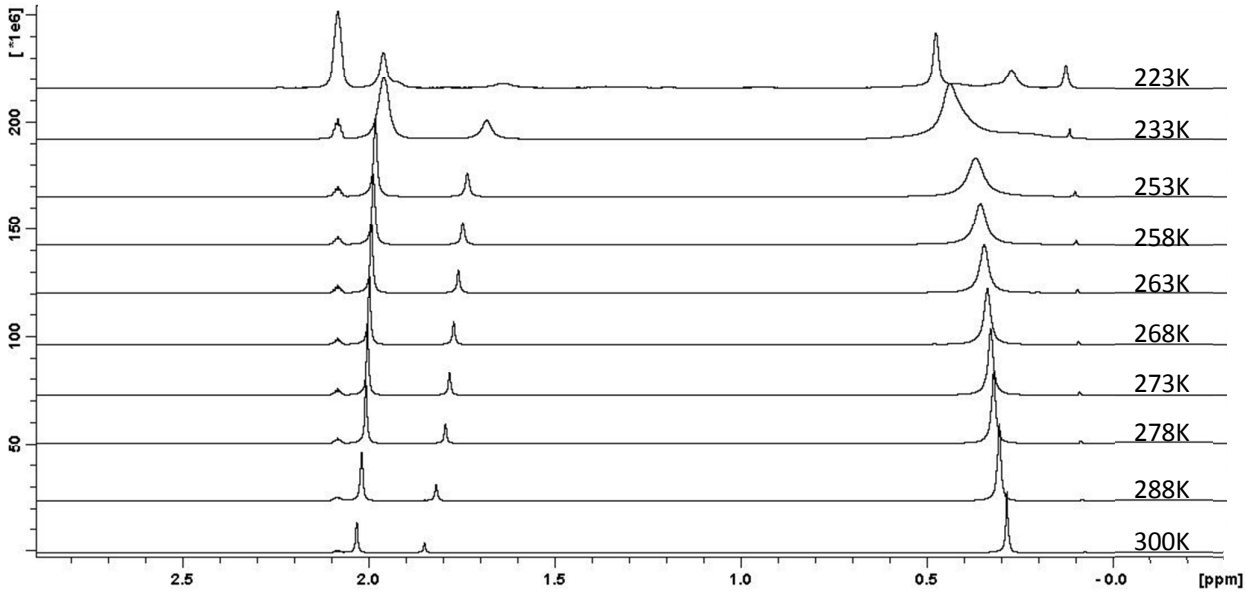

Figure S17. Variable temperature ^{1}H NMR spectra from 300 K to 223K (400.13 MHz, d_8-toluene) of isolated crystals of **7**. At 223 K (top spectrum) two distinct resonances at 0.47 and 0.27 ppm are present in a 2:1 ratio consistent with the HMDS ligands present in the solid state structure of **7**.

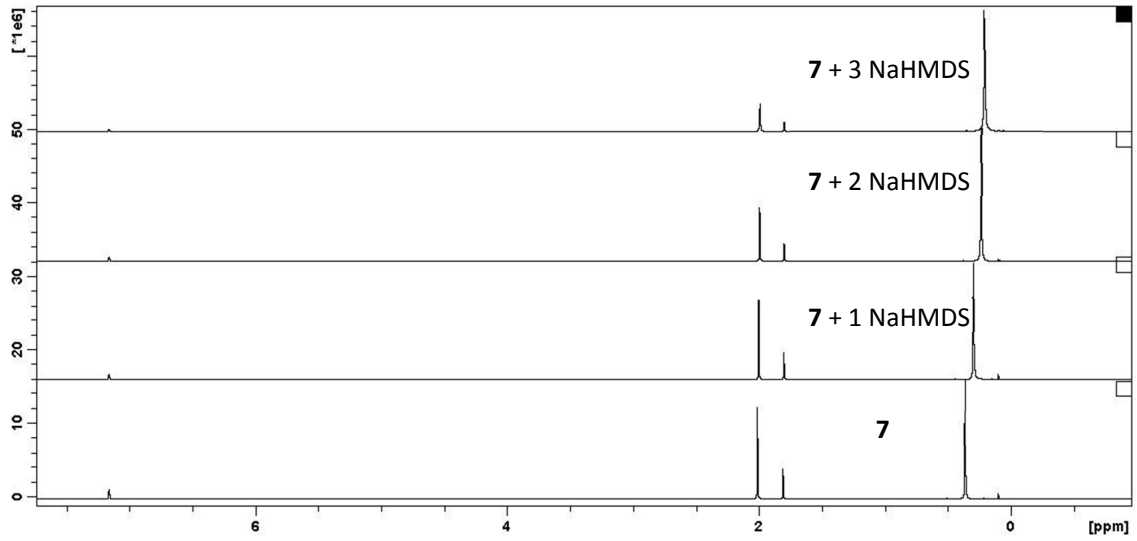

Figure S18. ^{1}H NMR spectra (400.13 MHz, C_6D_6) of isolated crystals of **7** (bottom), addition of 1 equivalent of NaHMDS to **7** (2nd bottom), addition of 2 equivalents of NaHMDS to **7** (2nd top) and addition of 3 equivalents of NaHMDS to **7** (top).

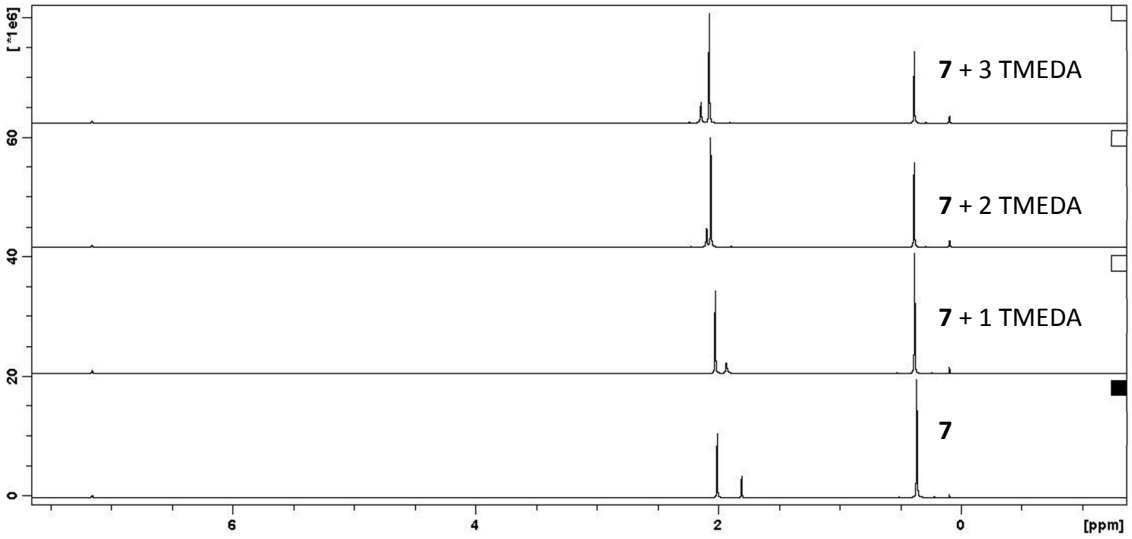

Figure S19. ^{1}H NMR spectra (400.13 MHz, C_6D_6) of isolated crystals of **7** (bottom), addition of 1 equivalent of TMEDA to **7** (2nd bottom), addition of 2 equivalents of TMEDA to **7** (2nd top) and addition of 3 equivalents of TMEDA to **7** (top).

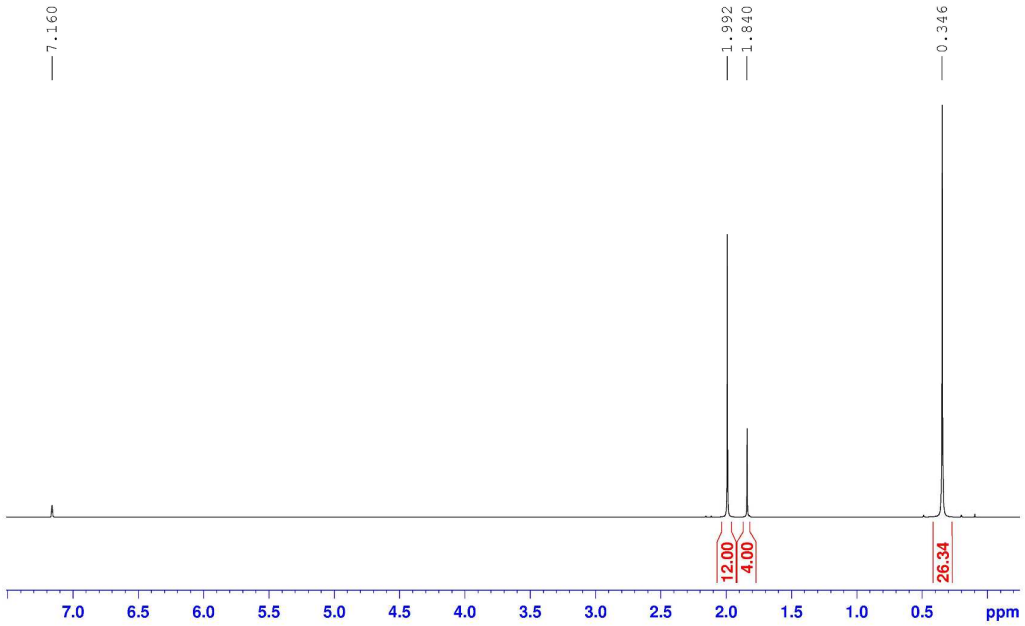

Figure S20. ^{1}H NMR spectrum (400.1 MHz, C_6D_6, 300 K) of isolated crystals of **8**.

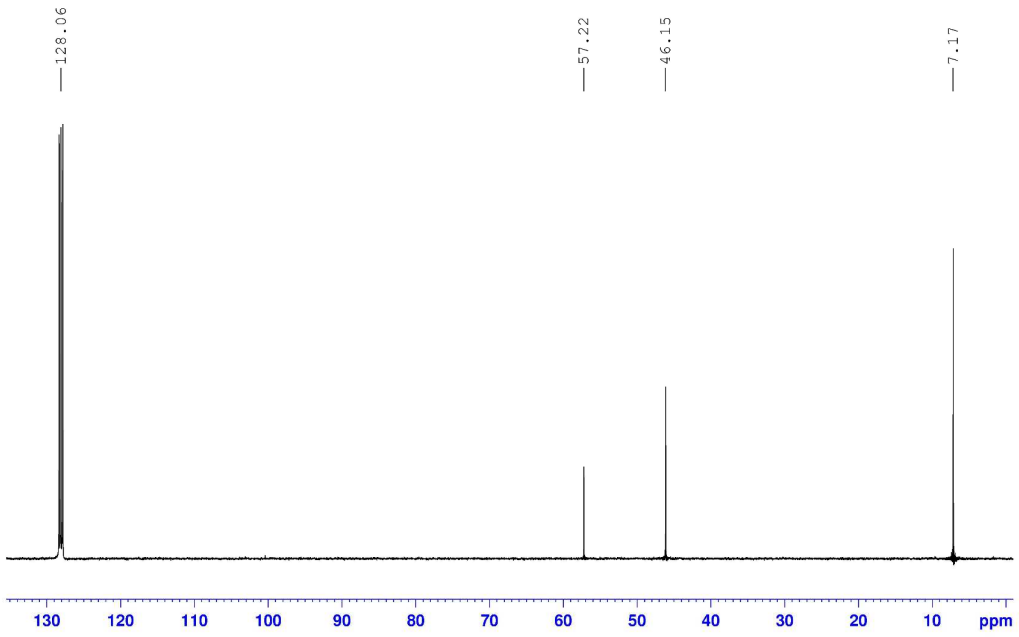

Figure S21. $^{13}C\{^{1}H\}$ NMR spectrum (100.6 MHz, C_6D_6, 300 K) of isolated crystals of **8**.

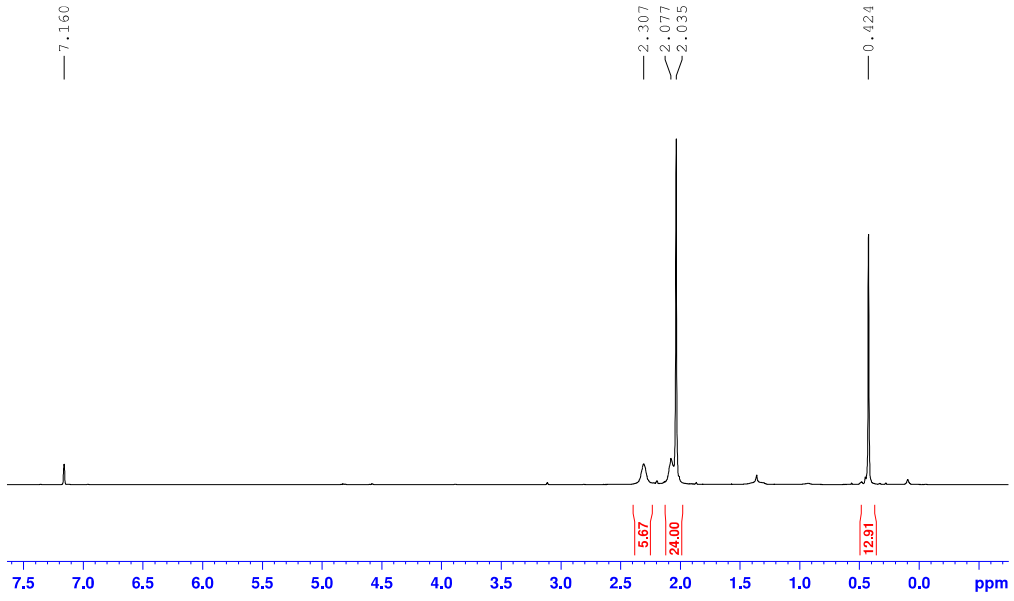

Figure S22. ^{1}H NMR spectrum (400.1 MHz, C_6D_6, 300 K) of **[(Me$_6$-TREN)Cs(HMDS)]**.

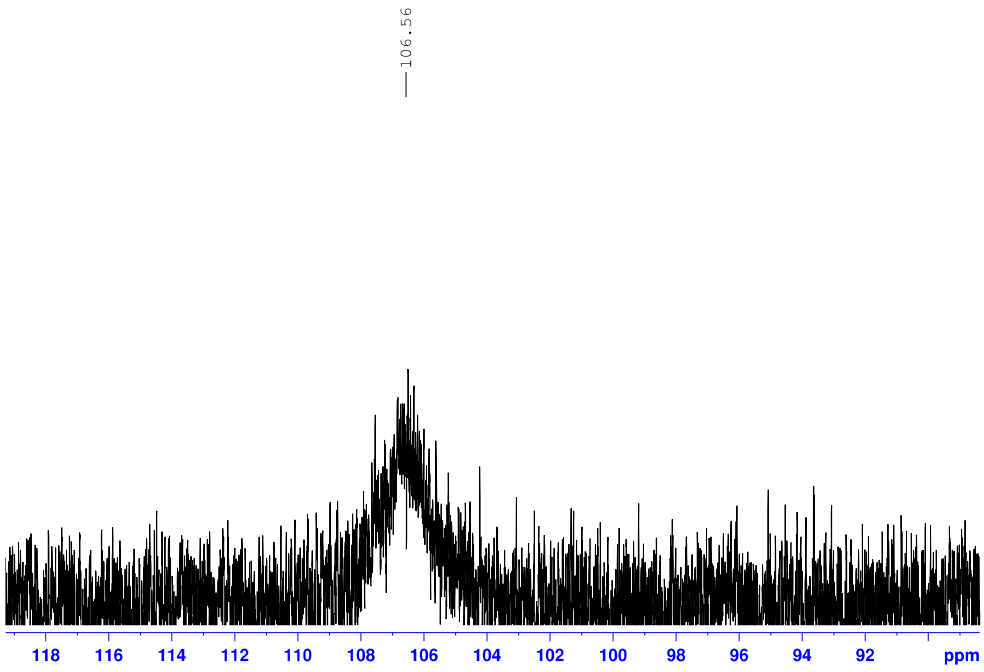

Figure S23. $^{133}Cs\{^{1}H\}$ NMR spectrum (52.5 MHz, C_6D_6, 300 K) of **[(Me$_6$-TREN)Cs(HMDS)]**.

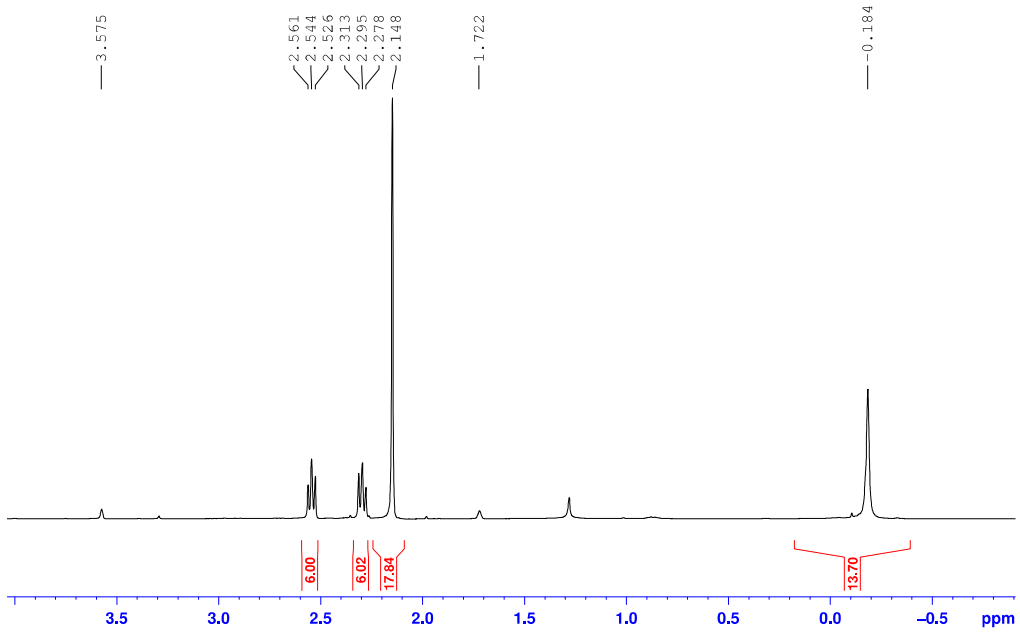

Figure S24. ^{1}H NMR spectrum (400.1 MHz, d_8-THF, 300 K) of **[(Me$_6$-TREN)Cs(HMDS)]**.

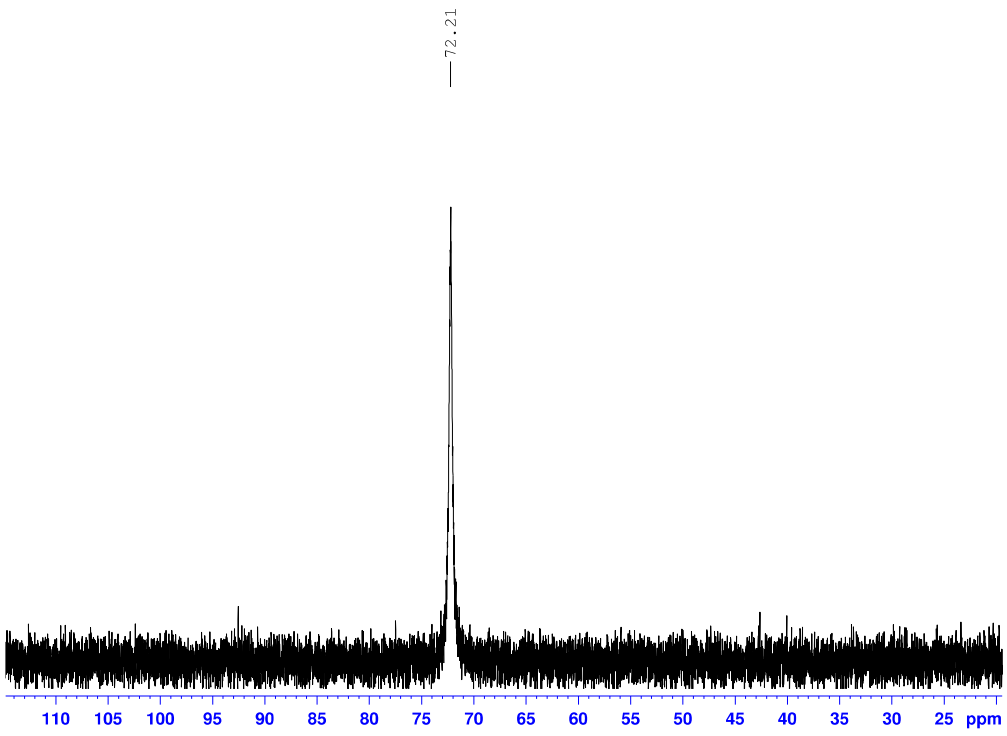

Figure S25. $^{133}Cs\{^{1}H\}$ NMR spectrum (52.5 MHz, d_8-THF, 300 K) of [(Me$_6$-TREN)Cs(HMDS)].

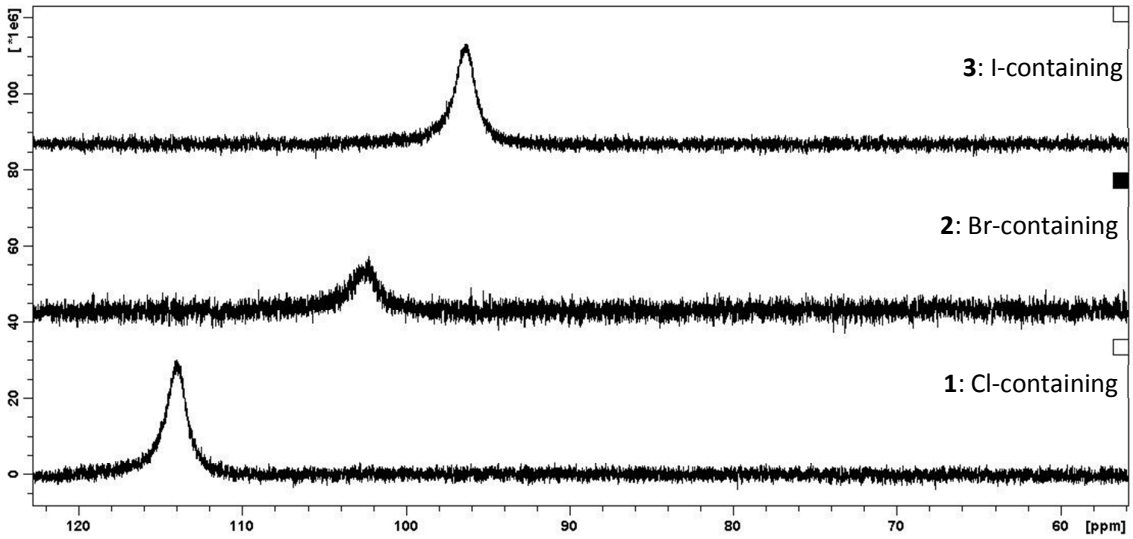

Figure S26. $^{133}Cs\{^{1}H\}$ NMR spectra (52.5 MHz, d_6-THF, 300 K) of aliquots of C_6D_6 solutions of **1**, **2** and **3** highlighting an upfield shift depending on the electronegativity of the halide ion in solution.